Check for updates

Received: 8 October 2022 | Accepted: 13 January 2023

DOI: 10.1002/pamm.202200286

Model order reduction via substructuring for a nonlinear, differential-algebraic machine tool model with moving loads

Quirin Aumann[1], **Peter Benner**[1,2], **Jens Saak**[1,2], and **Julia Vettermann**[1,*]

[1] Mathematics in Industry and Technology, Faculty of Mathematics, Technische Universität Chemnitz, Reichenhainer Str. 41, 09126 Chemnitz, Germany

[2] Computational Methods in Systems and Control Theory, Max Planck Institute for Dynamics of Complex Technical Systems, Sandtorstr. 1, 39106 Magdeburg, Germany

Machine tools are permanently exposed to complex static, dynamic and thermic loads. This often results in an undesired displacement of the tool center point (TCP), causing errors in the production process and thus limiting the achievable workpiece quality. Recent research efforts try to counter these effects by process-parallel solutions utilizing machine internal data. Therefore, fast simulation models are a fundamental requirement. Here, model order reduction (MOR) becomes crucial. The resulting low-dimensional models are required for various applications, e.g., in digital twins, the correction of thermally induced errors at the TCP during the production process as well as for lifetime calculations in predictive maintenance.
In this contribution, we present a strategy of MOR for a coupled thermo-mechanical model with a nonlinear subsystem and moving loads, using the example of a feed axis with nonlinear machine components. Applying tailored substructuring techniques, we are able to separate the linear and nonlinear system components. This allows to apply classic linear MOR methods to the much larger linear part, whereas the small nonlinear part is kept, and thus enables drastically reduced computing times. The relative movement is considered by a switched system approach. Transient thermo-mechanical interactions of the feed axis are calculated in a final investigation, comparing the performance of the resulting reduced-order model and the original one.

© 2023 The Authors. *Proceedings in Applied Mathematics & Mechanics* published by Wiley-VCH GmbH.

1 Outline

We will give a short introduction to the model in Section 2, and summarize the model order reduction (MOR) strategy for one pose in Section 3, since these topics are described in [14] in more detail. In this contribution, our MOR technique will be extended to systems with a relative movement between the subassemblies, which is handled by a switched system approach. Scaling effects play an important role in that context and will be discussed in Section 4.1. Numerical experiments and a short summary conclude this contribution.

2 Machine tool models with geometrically local nonlinearities

We consider the thermo-mechanical model of a subassembly of a modern 5-axis vertical milling machine described in [14]. It features two large structural parts, namely the slide and the headstock, and four machine components which are the carriages, see Figure 1. During the finite element (FE) analysis, the parts are modeled as linear elements, while the components are considered as nonlinear spring-damper elements using multi-point constraints. Here, the source of the nonlinearity is that a temperature change in the guideway systems of a machine tool can lead to a measurable change in the static stiffness. Therefore, the stiffness matrix has a small nonlinear part reflecting these geometrically local nonlinearities.

3 Model order reduction

The resulting system is represented as coupled differential-algebraic system Σ in generalized state-space form

$$\Sigma : \begin{cases} \begin{bmatrix} \mathbf{E}_{11} & \mathbf{0} \\ \mathbf{0} & \mathbf{0} \end{bmatrix} \begin{bmatrix} \dot{x}_1 \\ \dot{x}_2 \end{bmatrix} = \begin{bmatrix} \mathbf{A}_{11} & \mathbf{A}_{12}(t) \\ \mathbf{A}_{21}(t) & \mathbf{A}_{22}(x_2) \end{bmatrix} \begin{bmatrix} x_1 \\ x_2 \end{bmatrix} + \begin{bmatrix} \mathbf{B}_1 \\ \mathbf{B}_2 \end{bmatrix} u, \\ y = \begin{bmatrix} \mathbf{C}_1 & \mathbf{C}_2 \end{bmatrix} \begin{bmatrix} x_1 \\ x_2 \end{bmatrix}, \end{cases} \tag{1}$$

with the system matrices $\mathbf{E}, \mathbf{A} \in \mathbb{R}^{n\times n}$, the input map $\mathbf{B} \in \mathbb{R}^{n\times m}$, the output map $\mathbf{C} \in \mathbb{R}^{p\times n}$, the output $y \in \mathbb{R}^p$, the input $u \in \mathbb{R}^m$, and the states $x \in \mathbb{R}^n$, which include the temperature as well as the displacement and for the components also rotations around all three coordinate axes. While the states x_1 include the linear part of the system, the states x_2 contain the small nonlinear part. The coupling matrices $\mathbf{A}_{12}(t)$ and $\mathbf{A}_{21}(t)$ combine the linear and the nonlinear subsystem according

* Corresponding author: julia.vettermann@mathematik.tu-chemnitz.de

This is an open access article under the terms of the Creative Commons Attribution License, which permits use, distribution and reproduction in any medium, provided the original work is properly cited.

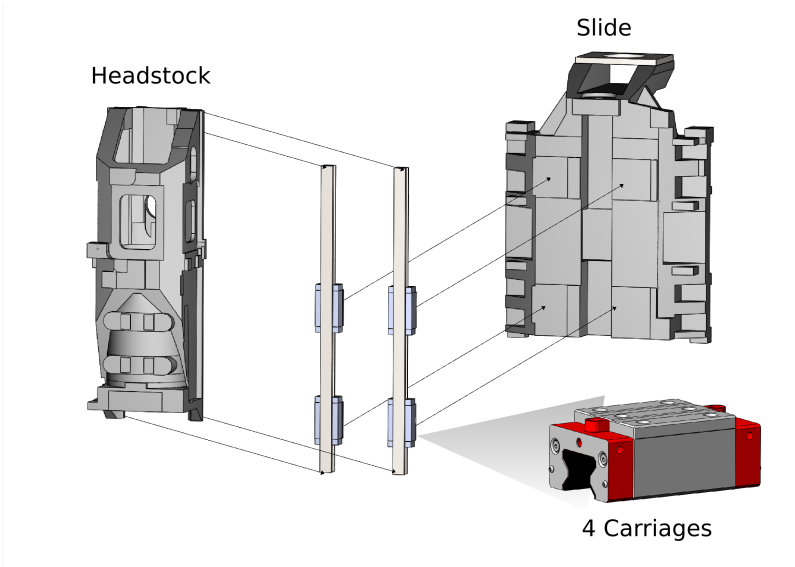

Fig. 1: Subassemblies of the feed axis model.

to the actual positioning of the subassemblies. Thus, we need an appropriate approximation of this time-varying effect to efficiently apply MOR. The strategy for the reduction of this system, with small nonlinear subsystem, for a fixed position is based on a sophisticated preprocessing technique including the decoupling of the linear and the nonlinear subsystems and the reduction of the large linear part with standard MOR methods for linear time-invariant (LTI) systems, see [14], while the small nonlinear part is kept. To obtain the coupled reduced-order model (ROM) $\tilde{\Sigma}$, the linear part is reduced by balanced truncation (BT), see e.g. [1, 4], and is afterwards recoupled with the nonlinear part. The decoupling is realized by a decomposition of the coupling matrices by an economy-sized singular value decomposition (SVD) utilizing the structural rank of the coupling blocks, such that we can individually treat the linear and nonlinear subsystem by the cost of additional inputs and outputs in both subsystems realizing the coupling between them. Note that the thermo-elastic system is modeled using a stationary linear elasticity model and thus the linear part is a differential-algebraic system of index 1 itself. Here an index-reduction is carried out and, provided that thermal and elastic DOFs use the same mesh and ansatz functions, already reduces the degrees of freedom (DOF) to $\frac{1}{4}$ of the original number of DOFs.

The resulting model is then further reduced by a system-theoretic MOR method. Thereby, truncation matrices $\mathbf{V}$ and $\mathbf{W} \in \mathbb{R}^{n\times r}$ are computed, restricting the model to an r-dimensional subspace with $r \ll n$, while the essential information on the input-to-output dynamics of the system is preserved. The ROM is obtained by

$$\tilde{\Sigma} : \begin{cases} \tilde{\mathbf{E}}\dot{\tilde{x}}(t) = \tilde{\mathbf{A}}\tilde{x}(t) + \tilde{\mathbf{B}}u(t), \\ \tilde{y}(t) = \tilde{\mathbf{C}}\tilde{x}(t) + \mathbf{D}u(t), \end{cases} \tag{2}$$

with the reduced matrices $\tilde{\mathbf{E}} := \mathbf{W}^\mathsf{T}\mathbf{E}\mathbf{V}$, $\tilde{\mathbf{A}} := \mathbf{W}^\mathsf{T}\mathbf{A}\mathbf{V}$, $\tilde{\mathbf{B}} := \mathbf{W}^\mathsf{T}\mathbf{B}$ and $\tilde{\mathbf{C}} := \mathbf{C}\mathbf{V}$, the reduced state $\tilde{x}(t) \in \mathbb{R}^r$ and the approximated outputs $\tilde{y}(t) \approx y(t) \in \mathbb{R}^p$. The additional feedthrough matrix $\mathbf{D}$ is resulting from the index reduction and includes a part of the information of the mechanical system.

3.1 Switched system approach

The MOR approach is expanded by the incorporation of the relative movement within the considered model. The structural variability in the model of the feed axis due to the relative movement leads to a time dependence of the coupling blocks $\mathbf{A}_{12}(t)$ and $\mathbf{A}_{21}(t)$ in (1). There exist different strategies to approximate a time-varying dynamical system in the field of MOR. The special case of MOR for coupled thermo-elastic linear systems with moving loads is investigated in [9]. We transfer the idea to consider the time-dependent movement in form of a switched system to our feed axis model. We define 6 poses and therefore end up with the switched system, illustrated in Figure 2, with 6 time-invariant switching modes Σ_α of the form (1) and a piecewise constant time-dependent switching signal $\alpha(t) : t \mapsto \mathcal{J} = \{1, \ldots, 6\}$, selecting the active switching mode at time t.

The switching modes are reduced separately according to the procedure described in [14], to receive an accurate local approximation of Σ_α for all $\alpha \in \mathcal{J}$. Therefore, the resulting local ROMs $\tilde{\Sigma}_\alpha$ may all use different subspace coordinates. In turn, additional state transformation matrices

$$\mathbf{T}_{\alpha^{+/-}} = \mathbf{W}_{\alpha^+}^\mathsf{T}\mathbf{E}\mathbf{V}_{\alpha^-} \tag{3}$$

© 2023 The Authors. *Proceedings in Applied Mathematics & Mechanics* published by Wiley-VCH GmbH.

16177061, 2023, 1, Downloaded from https://onlinelibrary.wiley.com/doi/10.1002/pamm.202200286 by MPI 335 Dynamics of Complex Technical Systems, Wiley Online Library on [12/06/2023]. See the Terms and Conditions (https://onlinelibrary.wiley.com/terms-and-conditions) on Wiley Online Library for rules of use; OA articles are governed by the applicable Creative Commons License

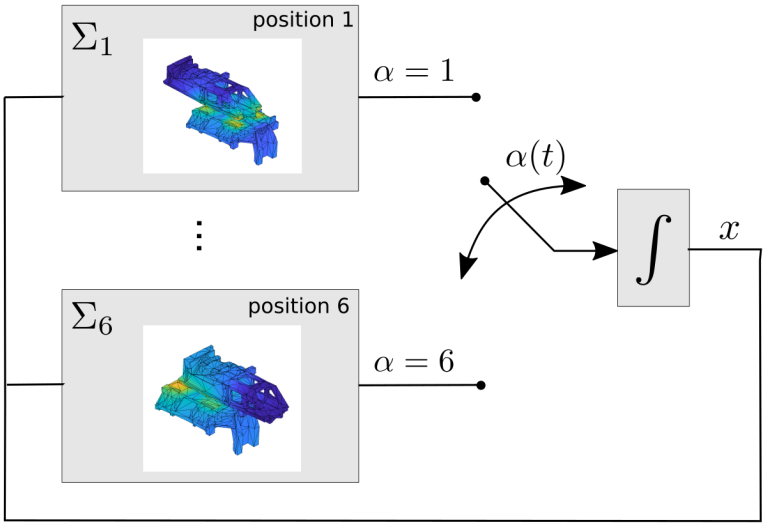

Fig. 2: Sketch of the switched system of the feed axis model with the switching modes Σ_α and the switching signal $\alpha(t)$.

are needed at the switching instances, to perform the realignment to the new coordinates of the reduced state in the new switching mode, i.e.

$$\tilde{x}_{\alpha^+}(t_s^+) = \mathbf{T}_{\alpha^{+/-}} \tilde{x}_{\alpha^-}(t_s^-) \tag{4}$$

with respect to the switching from the subspaces $\mathbf{V}_{\alpha^-}, \mathbf{W}_{\alpha^-}$ to $\mathbf{V}_{\alpha^+}, \mathbf{W}_{\alpha^+}$ at switching time t_s. In order to ensure a fast simulation of the switched system, the state transformation matrices should be precomputed during ROM creation in the so-called offline phase and stored with the ROMs. If we allow only the switching between neighboring switching modes, i.e. for neighboring rail segments, the storage requirements for these transformation matrices stay smallest possible. The more switching modes are used to represent the actual relative movement in the system, i.e. the shorter the rail segments are, the better is the approximation of the original system by the switched system. However, for a large number of modes the offline computation, which is required for the reduction process, becomes numerically expensive and the storage amount for the reduced modes and the generally combinatorially many state transformation matrices $\mathbf{T}_{\alpha^{+/-}}$ becomes prohibitive. Consequently, a reasonable number of switching modes is a prerequisite for an efficient reduction and simulation process. Furthermore, a suitable variant of balanced truncation for switched linear systems with constrained switching can be found in [7]. Also, for a switching between modes which are not neighbouring a multiplication of the state transformation matrices of the intermediate modes is possible to avoid the storage of all the transformation matrices. Therefore, let $\mathbf{T}_{ij}$ be the state transormation matrix from switching mode Σ_i to Σ_j. Then we have to multiply all intermediate neighboring transformation matrices, e.g., if we want to switch from switching mode 2 to 5 we get $\mathbf{T}_{25} = \mathbf{T}_{23}\mathbf{T}_{34}\mathbf{T}_{45}$.

Note that the stability of the individual systems in the switching modes Σ_α does not guarantee the stability of the overall switched system for an arbitrary switching signal $\alpha(t)$. For more information on the preservation of stability for switched systems, see e.g. [10, 11].

4 Numerical experiments

The systems in the switching modes were reduced by balanced truncation with tolerance 10^{-2}, see [14] for more details on the findings for a fixed position. The resulting reduced nonlinear switched system as well as the original one were simulated for a defined traversing profile of the feed axis. We allow only the switching between neighboring positions within the switched system. This requirement actually results in a restriction of the time step size by the feed speed. We use the traversing profile given in Table 2 for the simulation of the feed axis. The feed speed v leads to the maximal time step size $dt_{\max}$, given in the last column. The table also includes the start and end segment of the movement in the respective time interval, while the slide changes, the moving direction only when arriving in segment 1 or 6.

As quantity of interest, we want to examine the absolute z-displacement of the TCP, which directly affects the achievable working accuracy of the machine tool. A reliable approximation, especially of the TCP displacement, in the ROM is crucial for, e.g. real-time error correction of the thermally induced TCP error during the manufacturing process. The simulation was executed with the implicit Euler method for a time span of 100 s with a constant time step size of 0.1 s, thus we have a total number of 1 000 time steps. Table 1 shows a formidable speedup of the simulation time with the ROM while the reduced

 © 2023 The Authors. *Proceedings in Applied Mathematics & Mechanics* published by Wiley-VCH GmbH.

16177061, 2023, 1, Downloaded from https://onlinelibrary.wiley.com/doi/10.1002/pamm.202200286 by MPI 335 Dynamics of Complex Technical Systems, Wiley Online Library on [12/06/2023]. See the Terms and Conditions (https://onlinelibrary.wiley.com/terms-and-conditions) on Wiley Online Library for rules of use; OA articles are governed by the applicable Creative Commons License

Table 1: Comparison of reduction and simulation times t_{red} and t_{sim} for the switched system. (time step size: 0.1 s, 1000 time steps)

model	size	t_{red}	t_{sim}
switched system (FOM)	340 034	-	144 722 s $\sim$ 40 h
switched system (ROM, 6 switching modes)	207 | 206 | 207 206 | 206 | 208	2 145.4 s	3.4 s

Table 2: Traversing profile of the feed axis.

time interval in s	start	end	$\mathbf{v}$ in $\mathrm{m\,min^{-1}}$	$\mathbf{dt}_{\max}$ in s
$[0, 25]$	1	3	10	0.5136
$(25, 50]$	3	6	20	0.2568
$(50, 75]$	6	3	15	0.3424
$(75, 100]$	3	5	8	0.6420

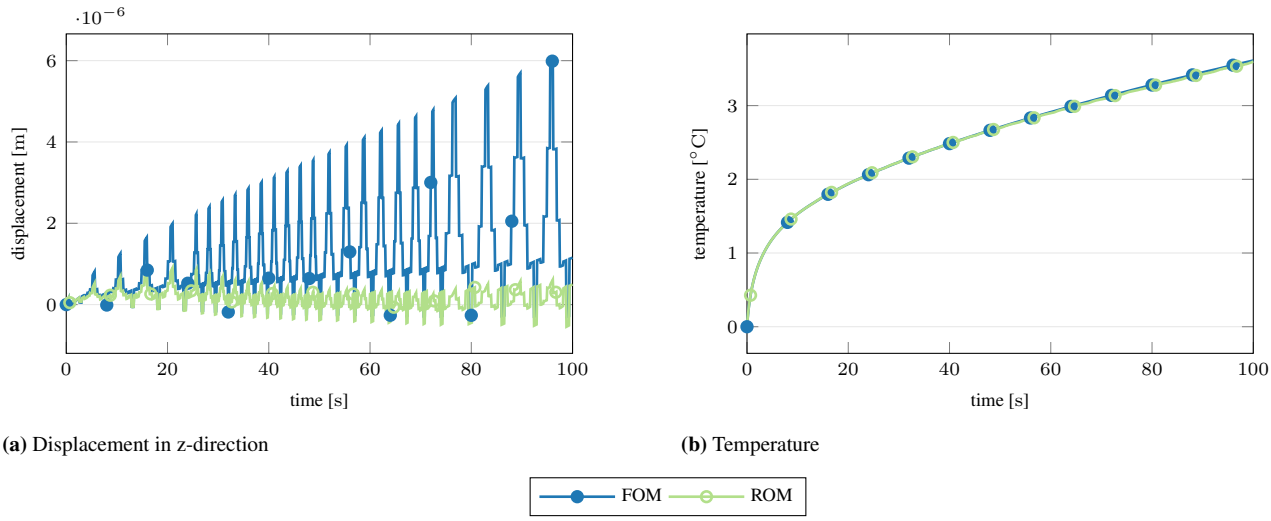

(a) Displacement in z-direction

(b) Temperature

Fig. 3: Comparison of the results for the FOM and the ROM at the TCP for the nonlinear switched system.

orders of the ROMs in the switching modes are between 206 and 208. As Fig. 3 shows, a sufficient accuracy with a relative error of order 10^{-1} can be achieved for the z-displacement in the switched system, the temperature results are even better. We see a good qualitative reproduction of the FOM trajectory with the ROM simulation in the displacement case. However, the quantitative deviation is not yet satisfying. At this point scaling effects come into consideration.

4.1 Scaling

In our numerical experiments, we also investigated the scaling of the model, because this might affect the quality of the ROM. In the original model, which was established in the commercial FE software ANSYS, standard units are used, i.e., $^\circ\mathrm{C}$ for the temperature and m for the displacement, although in the simulation we observe a displacement in the micrometer scale. So we have a large difference between the temperature and the displacement scales within the system. A scaling of the columns of $\mathbf{B}$ according to the magnitude of the corresponding inputs u could be beneficial, due to the fact, that the output error in time domain is also influenced by the norm of the input. An expression for the output error between the full and the ROM is obtained by

$$||y - \tilde{y}||_{\mathcal{L}_2} \leq ||\mathbf{H} - \tilde{\mathbf{H}}||_{\mathcal{H}_\infty} ||u||_{\mathcal{L}_2}, \tag{5}$$

with the transfer function $\mathbf{H} \in \mathbb{C}^{p \times m}[s]$, where

$$\mathbf{H}(s) = \mathbf{C}(s\mathbf{E} - \mathbf{A})^{-1}\mathbf{B}, \tag{6}$$

which describes the relation between the output response $\mathbf{Y}(s) = \mathbf{H}(s)\mathbf{U}(s)$ and the input signal $\mathbf{U}(s)$ of the system in frequency domain, while assuming a zero initial state, see, e.g. [2]. Also, a scaling of the rows of the output map $\mathbf{C}$ such that the magnitude of the outputs is of the same order can help to cope with the scaling problem. Due to the fact, that we get additional internal inputs and outputs in the model by the decoupling of the linear and the nonlinear subsystems, a scaling of the external input map $\mathbf{B}$ and output map $\mathbf{C}$ is not sufficient for the model at hand. Figure 4 shows the singular values (SV) of the output map of the original as well as the scaled linear subsystem after the decoupling and index-reduction and thus the

© 2023 The Authors. *Proceedings in Applied Mathematics & Mechanics* published by Wiley-VCH GmbH.

16177061, 2023, 1, Downloaded from https://onlinelibrary.wiley.com/doi/10.1002/pamm.202200286 by MPI 335 Dynamics of Complex Technical Systems, Wiley Online Library on [12/06/2023]. See the Terms and Conditions (https://onlinelibrary.wiley.com/terms-and-conditions) on Wiley Online Library for rules of use; OA articles are governed by the applicable Creative Commons License

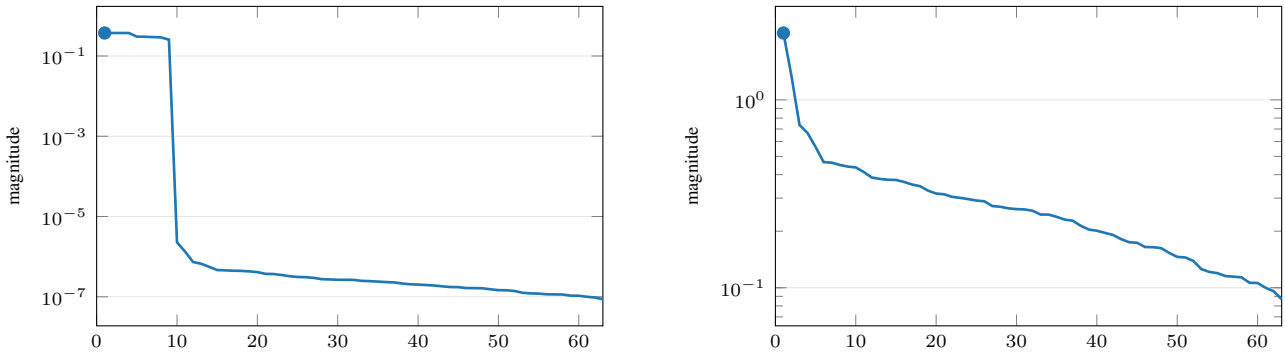

(a) Original system. **(b)** System scaled to micrometer.

Fig. 4: Comparison of the singular values of the original and the scaled output map used for the MOR of the index-reduced linear subsystem.

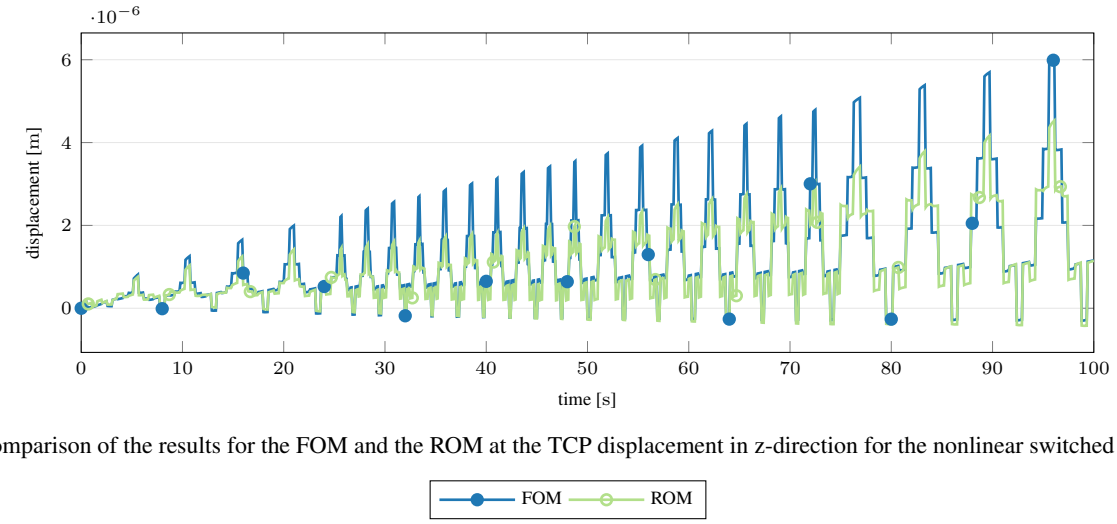

Fig. 5: Comparison of the results for the FOM and the ROM at the TCP displacement in z-direction for the nonlinear switched system.

additional internal outputs are included. We observe a large difference between the SV of the thermal and the elastic parts in the original model and thus the small ones belonging to the elastic states will play an inferior role during the reduction process, which can lead to larger reduction errors for the elastic DOFs.

Consequently, the whole system was scaled to micrometer to achive a balance between the magnitudes of the temperatures and displacement values in the model. The truncation tolerance was adapted to 10^{-6} to consider the properties of the scaled system and achieve a comparable reduced order of 208 to 210 in the switching modes. The simulation results in Figure 5, obtained with the scaled ROM, show a good approximation quality for the displacement in z-direction and can thus be applied as reliable surrogate in applications requiring fast simulations.

5 Future perspectives

The incorporation of inhomogeneous initial conditions in the MOR process is a further aspect which should be considered in the context of switched systems. It could be a potential cause for the remaining deviation of the ROM in Fig. 5. Although the overall process may start with zero initial conditions, we have to deal with nonzero initial conditions every time we switch into a different mode, i.e. due to the switch between the local systems and preservation of the current state. However, the system-theoretic MOR techniques, e.g., BT or moment matching methods, which aim at approximating the transfer function (6), rely on the assumption of a homogeneous initial condition, because there is no transient information included in the transfer function. Thus, the well-established BT error bound, see [1], is not guaranteed for such systems with nonzero initial conditions. Consequently, the low-dimensional subspaces generated by MOR have to be enriched by an appropriate representation of the initial condition. This can be achieved by adding an additional input matrix $\mathbf{E}\mathbf{X}_0$ and a related input $u_0(t) = z_0\delta(t)$ to the system, where $\delta(t)$ denotes the Dirac delta distribution and $\mathbf{X}_0 \in \mathbb{R}^{n\times n_0}$ spans a subspace $\mathbb{X} \subset \mathbb{R}^n$ which includes all possible initial values x_0 such that $x_0 = \mathbf{X}_0 z_0$ with $z_0 \in \mathbb{R}^{n_0}$. In [8], the input map $\mathbf{B}$ is directly extended by $\mathbf{E}\mathbf{X}_0$ prior to the reduction step, while the additional input is considered in a separate system in [3], which enables more adaptability in the reduction process. A new BT procedure for systems with nonzero initial conditions is proposed in [12] allowing a generalization of the two approaches outlined above.

 © 2023 The Authors. *Proceedings in Applied Mathematics & Mechanics* published by Wiley-VCH GmbH.

16177061, 2023, 1, Downloaded from https://onlinelibrary.wiley.com/doi/10.1002/pamm.202200286 by MPI 335 Dynamics of Complex Technical Systems, Wiley Online Library on [12/06/2023]. See the Terms and Conditions (https://onlinelibrary.wiley.com/terms-and-conditions) on Wiley Online Library for rules of use; OA articles are governed by the applicable Creative Commons License

The techniques, presented in [3, 8], were successfully applied to a thermal machine tool model with constant initial temperature for all nodes in [13]. In contrast to the application there, we have to deal with varying initial values in the nodes, due to the simulated machining process and the switching, here. In our application, we have no a priori knowledge about possible states at the switching instances, i.e. $\mathbf{X}_0$ spans the full space and thus would be the identity matrix. For such models with a large number of inputs special MOR techniques are required, e.g., BT for systems with many inputs presented in [5]. As a drawback, these methods produce an additional approximation error, due to a further outer approximation step. Furthermore, for the full temperature field as input, we have to approximate the full state by $x \approx \mathbf{V}\tilde{x}$, which is not necessarily accurate, since the MOR approach used here aims at finding a good approximation of the system outputs $y(t)$, i.e., the output error $||y(t) - \tilde{y}(t)||$ is small in a suitable norm. Thus, to achieve more accuracy it could be beneficial to choose the output map $\mathbf{C}$ as identity matrix. Such systems with many inputs and many outputs often arise in the field of power grid models. In [6] ESVDMOR, an extended MOR approach relying on an SVD, is discussed as MOR method of choice for these systems.

However, all these methods dealing with many inputs and/or outputs are very costly in terms of computation time and storage amount, for large-scale systems. Consequently, in our future research, we aim to find a suitable approximation of the subspace of all feasible initial values, which could be achieved, e.g., by utilizing a proper orthogonal decomposition (POD) with an adequate number of POD modes per input $u_i, i = 1, \ldots, m$, or the use of, potentially truncated, controllability subspace information of the other switching modes.

6 Conclusion

In this contribution, the strategy for MOR of a differential-algebraic machine tool model with geometrically local nonlinearities is extended to the case of moving loads which is realized by a switched system approach. While the simulation results with the ROMs for the single switching modes show a good qualitative match with the original models, see [14], in the switched system scaling effects have an impact on the quality of the ROM. By the choice of an appropriate scaling of the original model, the quality of the switched ROM could be improved. Hopefully, a further refinement of this model may be achieved by the incorporation of inhomogeneous initial conditions in the process of MOR in future investigations.

Acknowledgements Funded by the German Research Foundation – Project-ID 174223256 – TRR 96. Open access funding enabled and organized by Projekt DEAL.

References

[1] A. C. Antoulas. *Approximation of Large-Scale Dynamical Systems*, volume 6 of *Adv. Des. Control*. SIAM Publications, Philadelphia, 2005.

[2] U. Baur, P. Benner, and L. Feng. Model order reduction for linear and nonlinear systems: A system-theoretic perspective. *Arch. Comput. Methods Eng.*, 21(4):331–358, 2014.

[3] C. Beattie, S. Gugercin, and V. Mehrmann. Model reduction for systems with inhomogeneous initial conditions. *Systems & Control Letters*, 99:99–106, 2017.

[4] P. Benner, S. Grivet-Talocia, A. Quarteroni, G. Rozza, W. H. A. Schilders, and L. M. Silveira, editors. *Model Order Reduction. Volume 1: System- and Data-Driven Methods and Algorithms*. De Gruyter, Berlin, 2021.

[5] P. Benner and A. Schneider. Balanced truncation for descriptor systems with many terminals. *Preprint MPIMD/13-17, Max Planck Institute Magdeburg*, 2013.

[6] P. Benner and A. Schneider. Reduced representation of power grid models. In P. Benner, editor, *System Reduction for Nanoscale IC Design*, pages 87–134, Cham, 2017. Springer International Publishing.

[7] I. V. Gosea, I. Pontes Duff, P. Benner, and A. C. Antoulas. Model order reduction of switched linear systems with constrained switching. In J. Fehr and B. Haasdonk, editors, *IUTAM Symposium on Model Order Reduction of Coupled Systems, Stuttgart, Germany, May 22–25, 2018*, pages 41–53, Cham, 2020. Springer International Publishing.

[8] M. Heinkenschloss, T. Reis, and A.C. Antoulas. Balanced truncation model reduction for systems with inhomogeneous initial conditions. *Automatica*, 47(3):559–564, 2011.

[9] N. Lang, J. Saak, and P. Benner. Model order reduction for systems with moving loads. *at-Automatisierungstechnik*, 62(7):512–522, 2014.

[10] D. Liberzon. *Switching in Systems and Control*. Birkhäuser, Basel, 2003.

[11] I. Pontes Duff, S. Grundel, and P. Benner. New gramians for switched linear systems: Reachability, observability, and model reduction. *IEEE Transactions on Automatic Control*, 65(6):2526–2535, 2020.

[12] C. Schröder and M. Voigt. Balanced truncation model reduction with a priori error bounds for lti systems with nonzero initial value. *Journal of Computational and Applied Mathematics*, 420, 2023.

[13] J. Vettermann, S. Sauerzapf, A. Naumann, M. Beitelschmidt, R. Herzog, P. Benner, and J. Saak. Model order reduction methods for coupled machine tool models. *MM Science Journal*, 2021(3):4652–4659, 2021.

[14] J. Vettermann, A. Steinert, C. Brecher, P. Benner, and J. Saak. Compact thermo-mechanical models for the fast simulation of machine tools with nonlinear component behavior. *at - Automatisierungstechnik*, 70(8):692–704, 2022.

© 2023 The Authors. *Proceedings in Applied Mathematics & Mechanics* published by Wiley-VCH GmbH.

16177061, 2023, 1, Downloaded from https://onlinelibrary.wiley.com/doi/10.1002/pamm.202200286 by MPI 335 Dynamics of Complex Technical Systems, Wiley Online Library on [12/06/2023]. See the Terms and Conditions (https://onlinelibrary.wiley.com/terms-and-conditions) on Wiley Online Library for rules of use; OA articles are governed by the applicable Creative Commons License